Sains Malaysiana 53(6)(2024): 1343-1362
*http://doi.org/10.17576/jsm-2024-5306-10*

# Design and Characterisation of Curcumin-Loaded Nanostructured Lipid Carriers for Safe and Efficient Topical Drug Delivery in The Treatment of Pressure Ulcer

(Reka Bentuk dan Pencirian Pembawa Lipid Berstruktur Nano Berpengisi Kurkumin untuk Penghantaran Ubat Topikal yang Selamat dan Berkesan dalam Rawatan Ulser Tekanan)

NUR AMIRA MOHD SHAMSUDDIN[1], FAZREN AZMI[1], KHAIRANA HUSAIN[2], LEONG LEK MUN[3] & MOHD HANIF ZULFAKAR[1*]

*[1]Centre for Drug Delivery Technology & Vaccine, Faculty of Pharmacy, Universiti Kebangsaan Malaysia, 50300 Kuala Lumpur, Malaysia*
*[2]Centre for Drug and Herbal Development, Faculty of Pharmacy, Universiti Kebangsaan Malaysia, 50300 Kuala Lumpur, Malaysia*
*[3]Prima Nexus Sdn. Bhd., 28-1B, Jalan Puteri 1/2, Bandar Puteri, 47100 Puchong, Selangor, Malaysia*

*Received: 14 February 2024/Accepted: 16 May 2024*

ABSTRACT

Pressure ulcers (PU) are chronic lesions with a high prevalence in at-risk populations. Although curcumin has various therapeutic properties, its use as a dermal therapeutic agent is limited by its poor solubility and permeability. This study aimed to develop nanostructured lipid carriers (NLCs) to facilitate the topical use of curcumin as wound healing agent in treating PU. The optimised curcumin-NLCs were characterised for their physicochemical properties, drug release, and skin permeation, while effectiveness and toxicity were investigated via cell viability, scratch assays, and an *in vivo* skin irritation test. The optimised curcumin-NLCs comprised 3.5% solid lipids, 1% surfactant, and 2% co-surfactant with an average particle size of 134.68±6.0 nm, polydispersity index of 0.248±0.00, zeta potential of −44.94±5.44, percentage of encapsulation efficiency of 93.42±0.32%, and drug loading of 0.11±0.00%. Curcumin-NLCs showed stable physicochemical properties and extended drug release for up to 48 h, with a cumulative release of 77.72% following a first-order kinetics. The formulation exhibited slower curcumin permeation than the free curcumin. Furthermore, the safe and non-toxic curcumin-NLCs were highly effective at 0.98 μM and showed a high rate of wound closure without skin irritation. Collectively, the NLCs developed for topical delivery of curcumin demonstrated prolonged and sustained release and improved wound healing activity, which indicates that curcumin-NLCs are a viable strategy for treating PU.

Keywords: Curcumin; nanostructured lipid carrier; physicochemical characterisation; pressure ulcers; toxicity

ABSTRAK

Ulser tekanan (PU) adalah lesi kronik dengan prevalens yang tinggi dalam populasi berisiko. Kurkumin, walaupun mempunyai pelbagai sifat terapeutik, penggunaannya sebagai agen terapeutik kulit adalah terhad akibat keterlarutan dan kebolehtelapan yang lemah. Kajian ini bertujuan untuk membangunkan pembawa lipid berstruktur nano (NLC) untuk memudahkan penggunaan kurkumin sebagai ubat topikal untuk penyembuhan luka dalam merawat PU. Kurkumin-NLC yang dioptimumkan telah dicirikan berdasarkan sifat fizikokimia, pembebasan dadah dan penelapan kulit, manakala keberkesanan dan ketoksikan dianalisis melalui daya maju sel, asai penyembuhan luka dan ujian iritasi kulit *in vivo*. Kurkumin-NLC yang dioptimumkan terdiri daripada 3.5% lipid pepejal, 1% surfaktan dan 2% surfaktan bersama dengan saiz zarah purata 134.68±6.0 nm, indeks polidispersiti 0.248±0.00, potensi zeta −44.94±5.44, peratusan kecekapan pengkapsulan 93.42±0.32% dan pemuatan dadah 0.11±0.00%. Kurkumin-NLCs menunjukkan sifat fizikokimia yang stabil dan pembebasan ubat yang dilanjutkan sehingga 48 jam dengan pembebasan kumulatif sebanyak 77.72% mengikut kinetik urutan pertama. Formulasi menunjukkan penelapan kurkumin yang lebih perlahan

daripada kurkumin bebas. Tambahan pula, kurkumin-NLC yang selamat dan tidak toksik sangat berkesan pada 0.98 μM dan menunjukkan kadar penutupan luka yang tinggi tanpa iritasi kulit. Secara kolektif, NLC yang dibangunkan untuk penghantaran topikal kurkumin menunjukkan pembebesan yang berpanjangan dan berterusan serta aktiviti penyembuhan luka yang lebih baik, ini menunjukkan bahawa kurkumin-NLCs ialah strategi yang berdaya maju untuk merawat PU.

Kata kunci: Ketoksikan; kurkumin; pembawa lipid berstruktur nano; pencirian fizikokimia, ulser tekanan

## Introduction

A pressure ulcer, scientifically referred to as a decubitus ulcer or pressure injury, is a type of injury that affects the skin and underlying tissues. The phenomenon, also known as tissue necrosis, results from prolonged pressure, friction, shear, or a combination of these factors in localised regions of the body (Kottner et al. 2020). Restriction of blood supply to the affected area ultimately results in tissue death (Bhattacharya & Mishra 2015). Individuals who are immobile or have prolonged periods of limited physical activity, such as being wheelchair-bound or bedridden, the elderly, or those with chronic health conditions frequently develop pressure ulcers (Khor et al. 2014). In addition to causing physical discomfort and distress, pressure ulcers result in significant clinical complications such as osteomyelitis and sepsis (Khor et al. 2014), and managing pressure ulcers necessitates early intervention and prevention. Integrating an effective topical agent with conventional care interventions, such as regular patient repositioning, would yield ideal clinical results (Westby et al. 2015).

Curcumin, a polyphenolic compound, is extracted as a yellow-orange dye from the powdered roots (rhizomes) of turmeric (*Curcuma longa*) plants. It has been used for centuries in Ayurveda, Siddha, and traditional Chinese medicine owing to its potential therapeutic effects against various skin diseases, eye infections, dressings, and burns (Hatcher et al. 2008). Curcumin has been proven to have analgesic, anti-inflammatory, antioxidant, antiseptic, and anti-carcinogenic properties. Several studies have demonstrated the beneficial effects of curcumin on healing various types of wounds, including burns, surgical incisions, and diabetic ulcers. In the context of wound healing, curcumin effectively functions as an antibacterial agent during haemostasis; reduces inflammation; accelerates the proliferation process by enhancing re-epithelialisation; increases fibroblast proliferation, vascular density, collagen content, and granulation tissue formation; and facilitates wound contraction during remodelling (Akbik et al. 2014). However, its pharmaceutical significance is limited because of their hydrophobic nature, poor water solubility, low bioavailability, chemical instability, rapid metabolism, and short half-lives (Vijayakumar et al. 2019).

Various attempts have been made in recent years to overcome the challenges associated with the effective delivery of curcumin and enhance its wound-healing potential (Hussain et al. 2017). The use of nanostructured lipid carriers (NLCs) has been identified as a feasible strategy for overcoming these limitations (Borges et al. 2020). NLCs are lipid particles with a semi-solid hydrophobic lipid core and a hydrophilic exterior comprising both liquid and solid lipids and are stabilised by one or more surfactants (Esposito et al. 2014: Wissing, Kayser & Müller 2004). Owing to their high drug-loading capacity, biodegradability, biocompatibility, and ability to control drug release, these drug delivery systems exhibit promising potential for therapeutic applications (Haider et al. 2020). The different types, concentrations, and ratios of lipids and surfactants significantly influence the physicochemical properties and effectiveness of NLCs. This study aimed to design a drug delivery system utilizing NLCs to enhance the therapeutic efficacy of curcumin in wound healing for pressure ulcers employing glyceryl monooleate, olive oil, lecithin, and tween 80. In this study, the optimization variables of solid/liquid lipid, surfactant, and co-surfactant ratios of curcumin-NLC were designed by Central Composite Design (CCD). The optimized curcumin-NLCs were characterized based on particle size, polydispersity index and zeta potential, morphology, drug encapsulation, and loading capacity, DSC analysis, *in vitro* drug release/kinetic profile, and skin permeation study. The effectiveness of the curcumin-NLCs in wound healing was also investigated via cell viability and scratch assay in HaCat cell line.

## Materials and Methods

### Experimental design and optimisation

A Response Surface Methodology (RSM) generated using Design-Expert software (Version 13, Stat-Ease, Minneapolis, MN, USA) was used to optimise the NLC. A Central Composite Design methodology was utilised to investigate the interplay between the independent and dependent variables. The experimental factors considered in this study were the solid lipid composition ($X_1$) ranging from 3.5–4.75%, surfactant concentration ($X_2$) ranging from 1–3%, and co-surfactant concentration ($X_3$) ranging from 0.5–2%. The range in experimental factors was chosen based on preparation method from various published studies which used the highest and lowest composition of independent variable. The dependent variables were particle size ($Y_1$, in nm), polydispersity index (PDI) ($Y_2$), and zeta potential (ZP) ($Y_3$). The experimental design yielded 17 data points listed in Table 1. A linear model was utilised to analyse the correlation between independent variables and the dependent response.

$$Y = b_0 + b_1X_1 + b_2X_2 + b_3X_3$$

The dependent response variable, Y, was associated with a combination of factor levels. The formulation variables, namely particle size, PDI, and ZP, were used to express this relationship. The intercept is represented by $b_0$, and the regression coefficients of the respective variables are represented by $b_1$, $b_2$, and $b_3$. The statistical significance of the regression coefficients was assessed using p-values to determine the degree of correlation between the factors and the response variable. The suitability of the model were evaluated using an analysis of variance and the predicted $R^2$ value.

TABLE 1. Independent variables and responses for the 17-experiment formulation runs

| Formulation | Independent variable | | | Dependent responses | | |
|---|---|---|---|---|---|---|
| | $X_1$ (%) | $X_2$ (%) | $X_3$ (%) | $Y_1$ (nm) | $Y_2$ | $Y_3$ (mV) |
| 1 | 4.13 | 1.25 | 1.25 | 127.07 | 0.26 | -43.40 |
| 2 | 4.75 | 3 | 0.5 | 69.24 | 0.47 | -36.17 |
| 3 | 4.13 | 2 | 1.25 | 95.36 | 0.28 | -44.60 |
| 4 | 4.13 | 2 | 1.5 | 93.58 | 0.32 | -44.90 |
| 5 | 4.75 | 3 | 2 | 82.00 | 0.41 | -38.67 |
| 6 | 4.13 | 2 | 1 | 96.42 | 0.34 | -38.57 |
| 7 | 3.50 | 3 | 2 | 52.68 | 0.39 | -46.30 |
| 8 | 4.00 | 2 | 1.25 | 106.63 | 0.30 | -35.70 |
| 9 | 3.50 | 1 | 0.5 | 147.90 | 0.22 | -34.93 |
| 10 | 4.75 | 1 | 2 | 161.00 | 0.24 | -49.70 |
| 11 | 4.13 | 1.5 | 1.25 | 123.80 | 0.24 | -39.57 |
| 12 | 3.07 | 2 | 1.25 | 65.60 | 0.25 | -41.77 |
| 13 | 4.75 | 1 | 0.5 | 170.10 | 0.25 | -38.63 |
| 14 | 4.13 | 2.25 | 1.25 | 96.01 | 0.39 | -37.43 |
| 15 | 4.13 | 2.5 | 1.25 | 77.89 | 0.28 | -40.60 |
| 16 | 3.50 | 1 | 2 | 125.70 | 0.25 | -47.47 |
| 17 | 3.50 | 3 | 0.5 | 55.78 | 0.42 | -33.33 |

$X_1$, solid lipid; $X_2$, surfactant; $X_3$, co-surfactant; $Y_1$, particle size; $Y_2$, PDI; $Y_3$, ZP

### PREPARATION OF NLCS

The formulation of the NLC follows the formula established by the Design Expert software. Excipients comprising of a solid lipid, glyceryl monooleate (Dayang Chem, China), and a liquid lipid, specifically olive oil (Sigma-Aldrich, Germany), along with a surfactant, Tween 80 (Sigma-Aldrich, Germany), and a co-surfactant, lecithin (Acros Organic, Belgium), were utilised. NLCs containing curcumin were synthesised using high-shear and high-pressure homogenisation techniques. The liquid lipid content was quantified based on the weight of the solid lipids, using a 5% lipid phase ratio of solid to liquid lipids. The lipids were melted in a water bath maintained at a constant temperature of 70 °C. Subsequently, lecithin and 5 mg of curcumin were accurately weighed and blended with the lipid phase under magnetic stirring. The aqueous phase was prepared by dissolving Tween 80 in distilled water heated to 80 °C. The aqueous phase at a high temperature was rapidly dispersed into the lipid phase and homogenised using a high-shear homogeniser operated at 12,000 rpm for 20 min. The emulsion was then subjected to high-pressure homogenisation at 500 bars for three cycles. The experimental formulation runs were conducted at a constant homogenisation speed, duration, and cycle. The dispersion that was created underwent rapid cooling in a freezer set at 4 °C for 1 h before its storage or analysis.

### EVALUATION OF MEAN PARTICLE SIZE, POLYDISPERSITY INDEX, AND ZETA POTENTIAL OF THE OPTIMAL FORMULATION

The particle size distribution, PDI, and ZP were analysed via photon correlation spectroscopy using a Malvern Zetasizer (Nano ZS 90, Malvern Ltd., Malvern, UK). The samples were diluted 1:10 with double-distilled water to achieve an appropriate level of scattering intensity before the measurements were performed. The parameter values were acquired through backscatter at an angle of 173°, utilising disposable folded capillary cells at a temperature of 25 °C and allowing for 120 s of equilibration. A refractive index of 1.460 (with an absolute value of 0.01) was established for sizing the lipid NLC dispersions. ZP was determined by subjecting the sample to an electric field strength of 20 V/cm. The ZP value was calculated as the average of 30 measurements. All measurements were performed in triplicate.

### TRANSMISSION ELECTRON MICROSCOPY

Transmission electron microscopy (TEM; TALOS L120C, Thermo Fisher Scientific) was used to observe the morphology of nanoparticles. Curcumin-NLCs were diluted in distilled water and mixed by rotation. The samples were dropped on a copper grid coated with an amorphous carbon film and dried at an ambient temperature. The samples were observed at an operating voltage of 120 kV and analysed using the Velox (Thermo Fisher Scientific, US) software.

### DETERMINATION OF ENCAPSULATION EFFICIENCY (EE)

The encapsulation efficiency and drug loading of curcumin-NLCs were evaluated using an ultrafiltration technique. Initially, 100 µL of curcumin-NLCs were precipitated in 5 ml of acetonitrile (Merck, Germany) to facilitate the dissolution of the lipid shell and subsequent release of the curcumin entrapped within. Following centrifugation at 10,000 RPM for 30 min, the supernatant was collected to determine the total curcumin present in the formulation.

Subsequently, 500 µl curcumin NLCs was introduced into the top compartment of an Amicon ultrafilter and subjected to centrifugation at 4000 RPM for a duration of 30 min. Unencapsulated curcumin was acquired from the sediment at the base of the centrifugation tube. 100 µL of unencapsulated curcumin was collected and diluted with 5 mL of acetonitrile. A spectrophotometric analysis was performed at a wavelength of 426 nm. Curcumin concentration was determined using a calibration curve in an identical solvent mixture.

The EE% was calculated by dividing the weight of curcumin encapsulated by weight of total curcumin, where the weight of curcumin encapsulated indirectly equals the weight of the total drug minus the weight of unencapsulated drug. The equations used to calculate EE% were as follows:

$$\text{EE\%} = \left(\frac{Weight\ of\ total\ drug - Weight\ of\ unencapsulated\ drug}{Weight\ of\ total\ drug}\right) \times 100$$

The DL% was calculated by dividing the weight of encapsulated curcumin by the sum of the weight of curcumin and excipient. The weight of curcumin encapsulated indirectly equals the weight of the total drug minus the weight of unencapsulated drug, while the weight of excipient represents the total weight of solid lipid, liquid lipid, surfactant, and co-surfactant used. The equations used to calculate DL% were as follows:

$$\text{DL\%} = \left(\frac{Weight\ of\ total\ drug - Weight\ of\ unencapsulated\ drug}{Weight\ of\ total\ drug + Weight\ of\ excipient}\right) \times 100$$

### DIFFERENTIAL SCANNING CALORIMETRY (DSC) ANALYSIS

The NETZSCH DSC 214 was used to obtain thermograms of the NLC components, including GMO, olive oil, lecithin, and Tween 80, as well as blank NLC and curcumin-NLC. Most of the sample were semi solid (GMO and lecithin) and liquid (tween 80, olive oil blank NLC, and curcumin-NLC) in nature. Aluminium pans were used, and 20 mg of samples were hermetically sealed. The instrument was calibrated with indium. The temperature range for the NLC component was 25–100 °C, and the blank and curcumin-NLC were scanned at the same rate of 5 (°C /min) within the range of 25–225 °C (Puglia et al. 2012).

### STABILITY STUDY

The stability study was estimated by storing the optimised formulation at 4 °C and 25 °C for 30 days. Alterations in the particle size, PDI, and ZP content were determined to assess the stability of the formulation.

### *IN VITRO* DRUG RELEASE AND KINETICS

A drug release study of curcumin from the NLC formulations was conducted *in vitro* using the dialysis method to assess the behaviour of the drug within the formulation. The receptor medium used in this study was phosphate-buffered saline supplemented with 1% Tween 80 and 20% ethanol. A dialysis bag with a molecular weight cut-off of 14 KDa was filled with 1 mL of curcumin-NLCs. The dialysis bag was then placed in a beaker containing 200 mL of the receptor medium and subjected to magnetic stirring at 500 rpm. Samples from receptor medium were collected and replaced at specific time intervals of 15, 30, and 45 min and at 1, 2, 4, 6, 8, 24, and 48 h. A UV-Vis spectrophotometer was used to measure the absorbance at a wavelength of 426 nm in accordance with the standard calibration curve for curcumin in the receptor medium. The cumulative percentage of drugs released was then calculated. The release kinetics were determined by fitting the data to different kinetic models, including zero-order, first-order, Higuchi, Korsmeyer–Peppas, and Hixson–Crowell models.

### *IN VITRO* PERMEATION STUDIES

A study was conducted to evaluate the permeation *in vitro* using Franz diffusion cells. A cellulose acetate membrane with a pore size of 0.45 μm and diameter of 25 mm was inserted between the donor and receptor compartment. The experimental setup consisted of a receptor compartment with a volume of 5 mL and a contact area of 0.79 $cm^2$. The receptor compartment was filled with a cetrimide solution (30 mg/mL), which served as the receptor medium. The temperature of the receptor medium was maintained at 37 °C with stirring at 300 rpm. At specific time points (0.25, 0.5, 0.72, 1, 2, 4, 6, 8, 24, and 48 h), 0.5 mL samples were collected through the sampling port and replaced with fresh cetrimide solution to maintain a consistent volume of the receptor solution throughout the experiment. The samples were analysed using a UV-Vis spectrophotometer at a wavelength of 426 nm, in accordance with the standard calibration curve for curcumin in the receptor medium.

### CELL VIABILITY STUDIES

The HaCaT keratinocyte cell line, derived from adult humans with low calcium levels and high temperature, was procured from Addex Bio (San Diego, USA). Cells were cultured in Dulbecco's Modified Eagle Medium (DMEM) containing high glucose (4.5 g/L glucose), L-glutamine, and sodium pyruvate (Capricorn, Germany). The culture medium was supplemented with 10% foetal bovine serum (Capricorn, Germany) and 1% penicillin/streptomycin (Capricorn, Germany). HaCaT cells were seeded into 96-well plates at a cell density of $1 \times 10^5$ and incubated for 24 h in 100 μL DMEM. After incubation, the medium was replaced with a solution containing curcumin, curcumin-NLC, or blank NLC at concentrations ranging from 0.98–250 μM. The control group consisted of untreated cells, whereas the vehicle control group was treated with the same solvent used for curcumin dissolution (0.5% or 1% Dimethyl sulfoxide (Sigma-Aldrich, Germany)). The cells underwent an additional 24-h incubation period and were then subjected to Alamar blue (Bio-Rad) treatment. Cell analysis was performed using a UV-Vis spectrometer. The formula for determining the percentage of cell viability was as follows:

$$\text{Percentage of cell viability} = \left(\frac{Optical\ density\ of\ the\ sample}{Optical\ density\ of\ the\ negative\ control}\right) \times 100$$

### WOUND SCRATCH ASSAY

HaCaT cells were seeded into 24-well plates at a density of $2.5 \times 10^5$ per well. A monolayer of cells was scratched using a sterile 200 µL pipette tip and treated with various curcumin, curcumin-NLC and blank NLC concentrations in complete culture media. Untreated cells were used as negative controls. Images of the scratches were captured at 10x magnification using an inverted microscope immediately after the wounding procedure and repeated 24, 48, and 72 h later. The area of wound closure was measured using ImageJ software. Percentage wound closure was calculated using the following formula:

$$\text{closure} = \left(\frac{Area\ of\ the\ wound\ after\ scratching - Area\ of\ the\ wound\ at\ 24,48,or\ 72\ h\ after\ scratching}{Area\ of\ the\ wound\ after\ scratching}\right) \times 100$$

### SKIN IRRITATION TEST

The procedures were approved by the Animal Ethics Committee of the Universiti Kebangsaan, Malaysia, (FF/2021/MOHD HANIF/27-MAY/1181-OCT.-2022-OCT.-2023). Healthy female Sprague-Dawley rats weighing approximately 250 g were procured from the Laboratory Animal Resource Unit of the Universiti Kebangsaan Malaysia (UKM). The rats were fed a diet of standard pellets and allowed free access to water. During the experimental procedure, the rodents were exposed to regulated environmental conditions with a 12 h photoperiod cycle.

A skin irritation study was conducted using female Sprague–Dawley rats. The purpose of this test was to evaluate the irritation caused by the prepared curcumin-NLC on the intact skin of animals. After shaving the dorsal region of the rats, the treatment was applied to the tested area. Sodium lauryl sulfate was used as a positive control, normal saline was used as a negative control, and curcumin-NLC was used as the treatment. The test site was observed for erythema and oedema 24, 48, and 72 h after application. A primary skin irritation scoring system was used to evaluate the irritation. The absence of erythema or oedema in any of the formulations indicates that the prepared formulation will not cause skin irritation in animals (Gatne et al. 2015).

### STATISTICAL ANALYSES

Quantitative data are reported as mean ± SEM. All statistical measurements were analysed by Analysis of Variance (ANOVA) using SPSS (Version 22). Statistical significance was set at $p = 0.05$.

## RESULTS AND DISCUSSION

### EXPERIMENTAL DESIGN AND OPTIMISATION

Central composite design is an effective method for determining the optimal composition to achieve a specific target and represents the interaction among factors with a limited number of experiments (Behbahani et al. 2017). Table 1 lists the independent variables and responses for the 17-experiment formulation runs. The analysis of variance (ANOVA) for the linear model revealed that the entire model was significant. Figure 1 displays the 2D contour plots that show the influence of the factors on the responses of statistically significant variables to the analysed parameters. The particle size model's F-value of 77.10 suggests that the model is significant. $R^2$ was predicted to be 0.889 for $Y_1$. This implies that the independent variable accounted for 88.9% of the variation. The particle size ($Y_1$) is represented by the following formula, and the polynomial equations of the regression coefficients generated for the experimental data describe the relationships between the variables:

$$Y_1 = 103.16 + 14.97X_1 - 42.48X_2 - 2.75X_3$$

The response variable increased by positive unstandardised coefficients with an increase in the predictor, whereas the response variable decreased by negative unstandardised coefficients (Lakhani et al. 2018). The solid lipid content ($X_1$) and surfactant ($X_2$) had considerable effects on the effect of the factor levels on particle size, as shown in Figure 1(A) and the $Y_1$ equation, with large coefficients (14.97 and -42.38). This demonstrated that the particle size increased in direct proportion to the concentration of solid lipid. The increased viscosity of the lipid phase, which reduces the effectiveness of particle-breaking processes and the possibility of lipid coalescence with high concentrations of lipids, accounts for the favourable influence of SL% proportions on size (Castro et al. 2021; Emami et al. 2015). However, increased surfactant concentration led to a decrease in particle size. A surfactant was used to coat the nanoparticle surfaces to prevent agglomeration during homogenisation (Emami et al. 2015) and to decrease the interfacial tension between the nanoparticles and the external phase (Pradhan et al. 2015). Therefore, the particle size decreased as the

surfactant concentration increased (Bhatt et al. 2021). In this study, the ratio of solid lipids corresponded to that of liquid lipids when the amount of solid lipids increased, and that of liquid lipids decreased. Owing to the decrease in particle inner viscosity, the results indicated that the particle size decreased with an increase in the ratio of liquid lipids to total lipids (Yang et al. 2019).

The F-value for PDI was 17.48, indicating that the model was significant. The solid lipid, surfactant, and co-surfactant accounted for 68.08% of the fluctuation according to the adjusted $R^2$ value of $Y_2$ = 0.6808. This equation can be used to depict the model that explains the association between the independent variables and PDI ($Y_2$):

$$Y_2 = 0.3177+0.021X_1+0.0884X_2-0.0086X_3$$

The impact of the factor levels on the PDI was significantly affected by the surfactant, as indicated by a coefficient of 0.0884. An increase in the surfactant concentration resulted in a corresponding increase in PDI. Surfactants play a pivotal role in determining the size distribution of nanoparticles (Castro et al. 2021). The hydrophilic lipophilic balance (HLB) of a surfactant indicates relationship between hydrophilic and lipophilic properties of the non-ionic surfactants. As the surfactant HLB values increase the particle size and PDI increased (Housaindokht & Nakhaei Pour 2012). Surfactants at high concentrations can increase viscosity (Al-Waeli et al. 2019). Surfactants, also known as surface-active agents, are compounds that lower the surface tension of a liquid (Mulligan 2007). The reduction of surface tension allows the formation of smaller droplets, resulting in smaller mean nanoparticle sizes and PDI (Guhagarkar, Malshe & Devarajan 2009). Surfactants have a critical aggregation concentration (CAC) which is the concentration at which premicellar aggregates form (Szutkowski et al. 2018). The increase in the PDI can also result from rapid coalescence or the presence of nanoparticles or micelles (Soleimanifard et al. 2020).

To satisfy the assumptions of the linear model for ANOVA, the $Y_3$ response variable was transformed using inverse linear regression. Statistical analysis indicates that the model is significant, as evidenced by the model F-value of 9.06 for ZP. The predicted $R^2$ value of 0.4070 was in reasonable agreement with the adjusted $R^2$ value of 0.6017. This suggests that 40.7% of the observed differences in the dependent variable can be explained by changes in independent variables. The equation for the independent variables of 1/ZP ($Y_3$) is as follows:

$$1/Y_3 = -0.0249+0.0001X_1-0.0012X_2+0.003X_3$$

Based on this equation and Figure 1(C), it is evident that the co-surfactant affects the ZP of the NLCs. This finding highlights the significant role of co-surfactants in determining the ZP of curcumin-NLCs. Specifically, an increase in the concentration of the co-surfactant led to a corresponding increase in the ZP. The ZP values exhibited a decrease in negativity with an increase in the amounts of lecithin. This can be attributed to the stronger anionic surface charge induced by lecithin, thus reducing the negatively charged surface (Chuacharoen, Prasongsuk & Sabliov 2019).

## EVALUATION OF MEAN PARTICLE SIZE, POLYDISPERSITY INDEX, AND ZETA POTENTIAL OF THE OPTIMAL FORMULATION

Table 2 presents a comparison of the predicted and experimental data means under the optimal conditions for the final formulation, comprising of 3.5% solid lipids, 1% surfactant, and 2% co-surfactant. These values were obtained by imposing constraints on the desired values of the dependent variables. The optimisation criteria for achieving a particle size below 200 nm, a PDI below 0.3, and a ZP within the range of -30 to -50 resulted in a solution with a desirability score of 0.347. The experimental results for the curcumin-NLCs showed that the predicted values of particle size, PDI, and ZP were in close agreement with the actual values, with a less than 5% variation. This indicated that the optimised formulation was reliable and acceptable. The curcumin-NLCs showed no significant differences in terms of particle size, PDI, and ZP compared to the blank NLC. Nanoparticle size is a crucial attribute affecting both drug release kinetics and absorption patterns (Gazori et al. 2009). Curcumin-NLCs with an average diameter below 200 nm have the potential to facilitate drug penetration into the skin, thereby improving topical drug delivery. The homogenous distribution of particle sizes in the curcumin-NLC was confirmed by the low PDI values. A PDI value greater than 0.3 signifies a significant level of heterogeneity in particle size and a wide distribution. Conversely, a lower PDI value indicates a uniform particle size distribution (Elmowafy et al. 2016). Zeta potential reflects the stability of the colloidal system. It represents the repulsive force between

a)

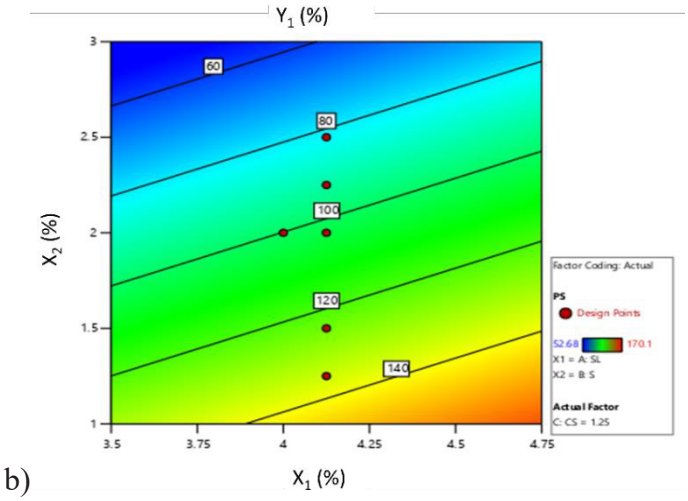


b)

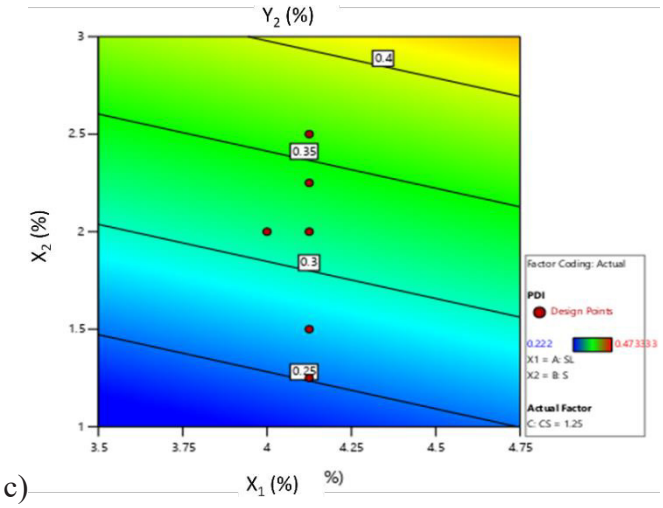


c)

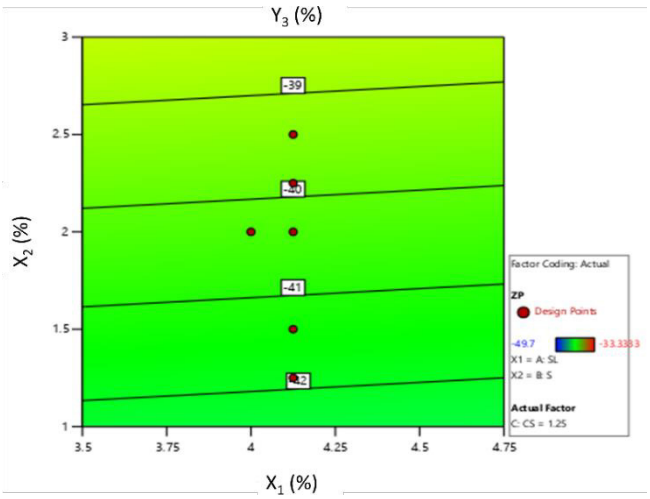


FIGURE 1. 2D contour plots showing the influence of the factors on the responses of the statistically significant variables to the analysed parameters. a) Particle size ($Y_1$) b) PDI ($Y_2$) c) ZP ($Y_3$)

particles with comparable charges in the formulation and how the repulsive forces prevent the particles from aggregating during storage (Das, Ng & Tan 2012). For full electrostatic stabilisation, the zeta potential should be equal to or greater than -30 mV (Rahman et al. 2013). The highly negative charge of the zeta potential of the curcumin-NLCs suggest that the nanoparticles exhibit a high degree of stability. The negative zeta potential is due to the dissociation of fatty acids from the NLC (Kumbhar & Pokharkar 2013). Liquid lipids typically exhibit a high degree of dissociation from incorporated fatty acids. The presence of liquid lipids reduces the surface area of the NLCs, leading to an increase in the zeta potential of the lipid system (Nahak et al. 2016).

### TRANSMISSION ELECTRON MICROSCOPY

Figure 2 depicts the morphology of curcumin-NLCs observed by TEM. TEM images illustrate that the particles in the curcumin-NLC dispersion are uniformly spherical and homogeneously distributed, with a mean diameter of 131.48±3.43 nm. The TEM micrograph of curcumin-NLCs shows a particle size slightly similar to that observed by photon correlation spectroscopy. The morphology obtained by TEM in this study resembles that reported by Kamel, Fadel and Louis (2019). The dark and dense core components of the particles appear to represent curcumin and a semi-solid hydrophobic lipid core consisting of GMO and olive oil. The loose grey external structure may represent a hydrophilic exterior comprising the surfactant and co-surfactant, which consist of Tween 80 and lecithin, respectively.

TABLE 2. Comparison of predicted and experimental data means under optimal conditions for the final formulation

| Analysis | Predicted Mean | 95% PI low | Data Mean (n=4) | | 95% PI high |
|---|---|---|---|---|---|
| | | | Blank NLC | curcumin-NLC | |
| PS (nm) | 127.92 | 112.65 | 125.43±11.58 | 134.68±6.0 | 143.19 |
| PDI | 0.2 | 0.14 | 0.248±0.05 | 0.25±0.00 | 0.26 |
| ZP (mV) | -48.49 | -56.34 | −45.8±3.63 | −44.94±5.44 | -42.01 |

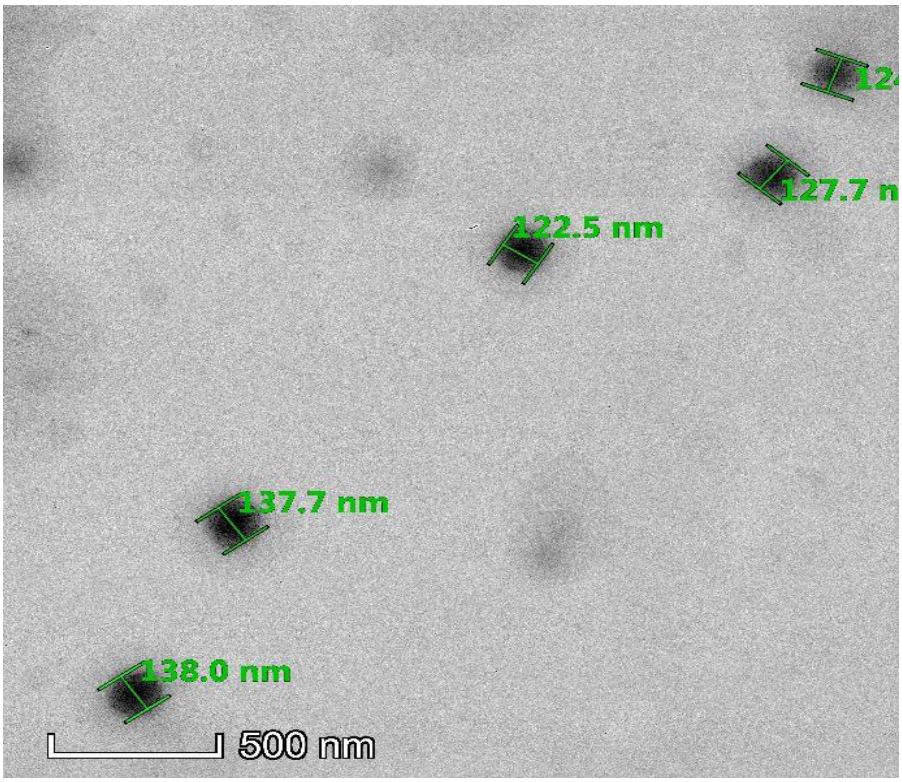


FIGURE 2. Morphology of curcumin-NLCs observed by transmission electron microscopy (TEM)

### THE MEAN PERCENTAGE OF ENCAPSULATION EFFICIENCY AND DRUG LOADING

The mean EE% and DL% values for curcumin-NLC dispersion were determined to be 93.42±0.32% and 0.11±0.00%, respectively. As the liquid-to-solid lipid ratio increases, the encapsulation efficiency of the nano-carriers also increases, owing to the enhanced solubility of the encapsulation material in the liquid lipid. Incorporating liquid lipids into solid lipids leads to the formation of nano-carriers in a less crystalline and more amorphous state. This process ultimately resulted in the formation of defects in the crystal lattice and increased encapsulation materials within the nano-carriers, thereby enhancing the efficacy of encapsulation and drug loading (Soleimanifard et al. 2020).

### DSC ANALYSIS

Thermographic analysis indicated that the components of NLC in the form of nanoparticles resulted in a broader endothermic peak. GMO displayed an endothermic peak at a temperature of 41.6 °C, olive oil exhibited a peak at 58.9 °C, lecithin showed a peak at 92.7 °C, and Tween 80 displayed a peak at 59.4 °C. Notably, curcumin demonstrated a high endothermic peak, above 100 °C. The blank NLC exhibited an endothermic peak at a temperature of 103 °C. In contrast, the curcumin-NLCs displayed an increase in the endothermic peak at a temperature of 108.3 °C. This outcome implies that curcumin can be integrated into the lipid matrix of the NLC, leading to a broader peak.

### STABILITY STUDY

This study aimed to determine the physical behaviour and evaluate the expulsion for short-term storage stability of optimal curcumin-NLCs at 4 °C and 25 °C. Throughout the storage period, there was no statistically significant variation in particle size, PDI, or ZP compared to the initial measurements on day 0. The curcumin-NLC exhibited consistent physical and physicochemical characteristics at both temperatures and provided a particle size of less than 200 nm, PDI of less than 0.5, and ZP within the range of -30 to -50.

### *IN VITRO* DRUG RELEASE AND KINETIC DRUG RELEASE STUDY

Dialysis was employed to evaluate the *in vitro* drug release kinetics of curcumin-NLCs compared to curcumin solutions, as shown in Figure 3. Maximum drug release was observed at 48 h for both formulations. The drug release percentages for the curcumin-NLCs and curcumin solution were 77.72% and 51.74%, respectively. The drug release pattern exhibited a characteristic biphasic behaviour. Within 1 h, approximately 13.66% of curcumin was released. The rapid release of curcumin was expected because of the drug-enriched shell model, which causes the release of the drug that is adsorbed on the surface of the nanoparticles (Liu, Wen & Sharma 2020). Furthermore, because of the small particle size of the curcumin-NLCs, they have a wider surface-to-volume ratio, which stimulates burst release (Sreedharan & Singh 2019). The drug was released, followed by sustained release kinetics for 2–48 h. Controlled-release systems are crucial for achieving both a rapid initial burst for therapeutic effect and a sustained release to maintain desired drug concentration over time (Sreedharan & Singh 2019).

To evaluate the mechanism of drug release by the curcumin-NLC, *in vitro* drug release was fitted to different kinetic models. The best-fit model was selected based on the highest correlation coefficient ($R^2$). Based on the release kinetics analysis, the release data were best fitted to first-order, with an $R^2$ value of 0.973. This suggests that the drug release rate was dependent of the drug concentration (Sreedharan & Singh 2019). The amount of drug released increased linearly over concentration at a constant release rate. The release data were fitted using the Korsmayer–Peppas equation to confirm the diffusion-controlled mechanism. In the Korsmeyer–Peppas model, the release exponent (n) defines the release mechanism. In this study, the corresponding plot for the Korsmeyer–Peppas equation also showed good linearity. The release exponent 'n' was found to be 0.3692, which less than 0.43, which indicates a Fickian diffusion drug release mechanism (Liu, Wen & Sharma 2020). The good linearity of the Hixson–Crowell model suggests a contribution of dissolution alongside diffusion, likely due to the changing surface area and diameter of the particles as they release the drug.

### *IN VITRO* PERMEATION STUDIES

An *in vitro* permeation study was performed to determine the permeation of curcumin from the formulations into the skin. The cumulative amount of curcumin permeated through the surface area for Curcumin-NLC, and curcumin solution were 2.12 μg/cm² and 10.51 μg/cm², respectively. The permeation of curcumin from the NLC into the skin exhibit a slow and sustained drug release mechanism. This signifies a controlled and gradual release of the drug, holding the potential to mitigate adverse effects and preventing toxicity. Maintaining therapeutic concentrations for extended periods can improve the efficacy of drugs,

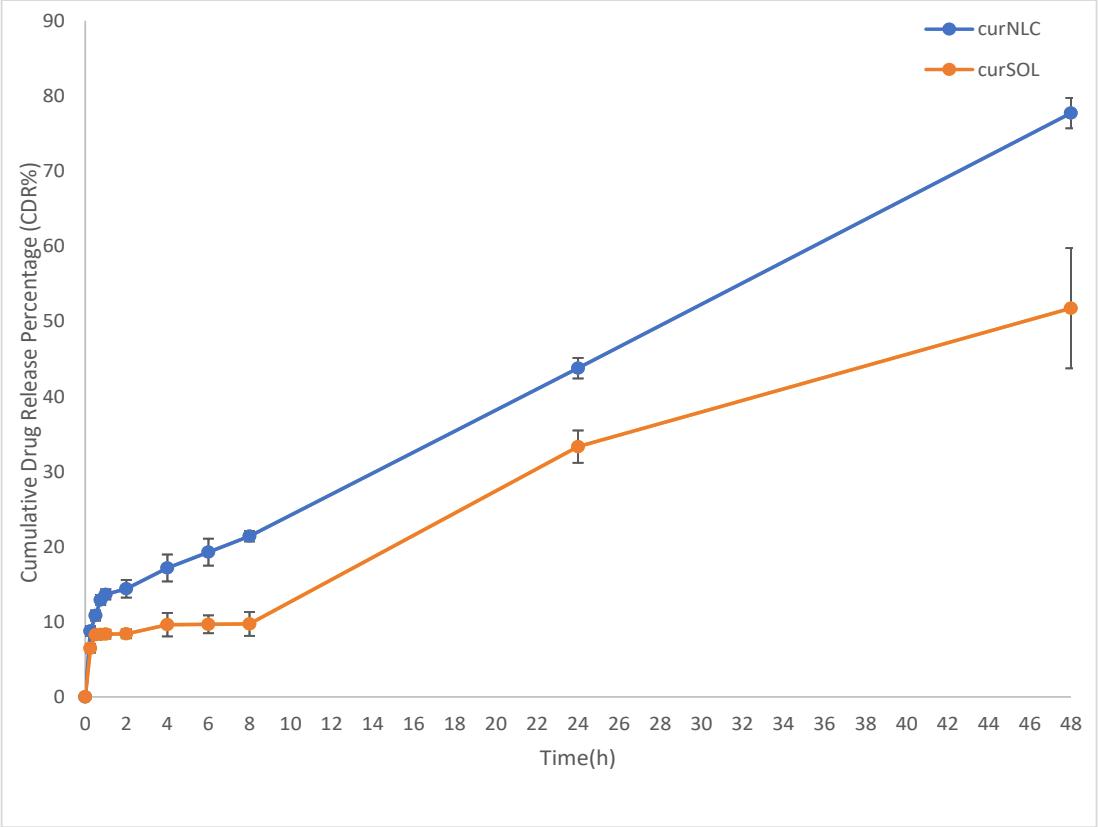


FIGURE 3. *In vitro* drug release profile of curcumin solution and curcumin-NLC dispersion (Mean ± SEM, n= 3)

thereby enhancing their potency and duration of action while reducing the need for higher and more frequent dosages.

## CELL VIABILITY STUDIES

An *in vitro* cell viability assay was conducted to determine the safe dose and compare the effects of curcumin, blank-NLC and curcumin-NLCs on the viability of HaCaT cells. Figure 4 shows the effect of curcumin, blank-NLCs, and curcumin-NLCs on HaCaT cell viability when treated with concentrations ranging from 0.98 to 250 µM. Compared to the untreated control, curcumin-NLC showed a significant increase in cell viability of more than 100% at 0.98–1.95 µM. Notably, no significant cytotoxicity was observed for any formulation at concentrations between 0.98 and 15.63 µM. However, a significant reduction in cell viability (less than 50%), was observed at concentrations of more than 62.5–125 µM for both blank and curcumin-NLC formulations. This is in agreement with Rapalli et al. (2020) who reported that curcumin-NLC dispersion and pure curcumin solution at a dose concentration of 40 µM or higher in the HaCaT cell lines mediated a decrease in cell viability by more than 50%. To sum up, the curcumin-NLC exhibited an impact similar to that of pure curcumin, and significantly improved cell viability against the HaCaT cell line compared to blank NLC, up to a certain concentration.

## WOUND SCRATCH ASSAY

Concentrations ranging from 0.98 to 31.25 µM, which exhibited no cytotoxicity on HaCaT cells were used in a wound scratch assay to assess cell migration and wound closure percentage. Results indicate that wound scratch closure over time is directly proportional to the concentration. The curcumin-NLC at a concentration of 0.98 µM exhibited a significantly higher wound closure rate than the control group at 24 h. All concentrations ranging from 0.98–15.21 µM exhibit complete wound closure after 48 h compared to the control. However, a significant reduction in wound closure rate was observed at a concentration of 31.25 µM. The rate of wound closure at this higher concentration was lower compared to untreated, indicating slower cell migration with higher concentrations. Curcumin is known to modulate various

cellular pathways crucial for wound healing. While lower doses might positively influence these pathways, exceeding a certain threshold could disrupt the delicate balance, leading to impaired healing, or disruption of cell signalling (Akbik et al. 2014; Toden et al. 2015). Figure 5 shows a comparison between curcumin-NLC with curcumin and blank NLC on wound closure of HaCaT cells treated with 0.98–31.25 µM at 24, 48,

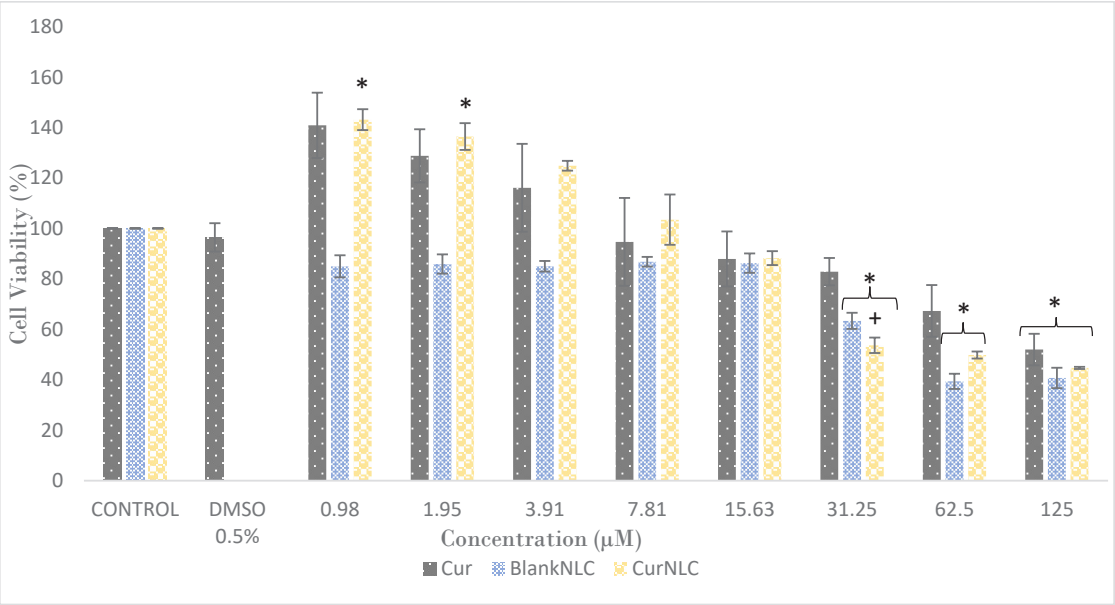


FIGURE 4. Effect of curcumin, blank NLCs, and curcumin-NLCs on HaCaT cell viability treated at 250–0.98 µM. *Statistically significant (one-way ANOVA, Tukey's post hoc test, $p<0.05$) compared with the respective controls. Data expressed as n=4 ±SEM. # Statistically significant (one-way ANOVA, Tukey's post hoc test, $p<0.05$) against the respective concentration of curcumin. +Statistically significant (one-way ANOVA, Tukey's post hoc test, $p<0.05$) against the respective concentrations of Blank NLC

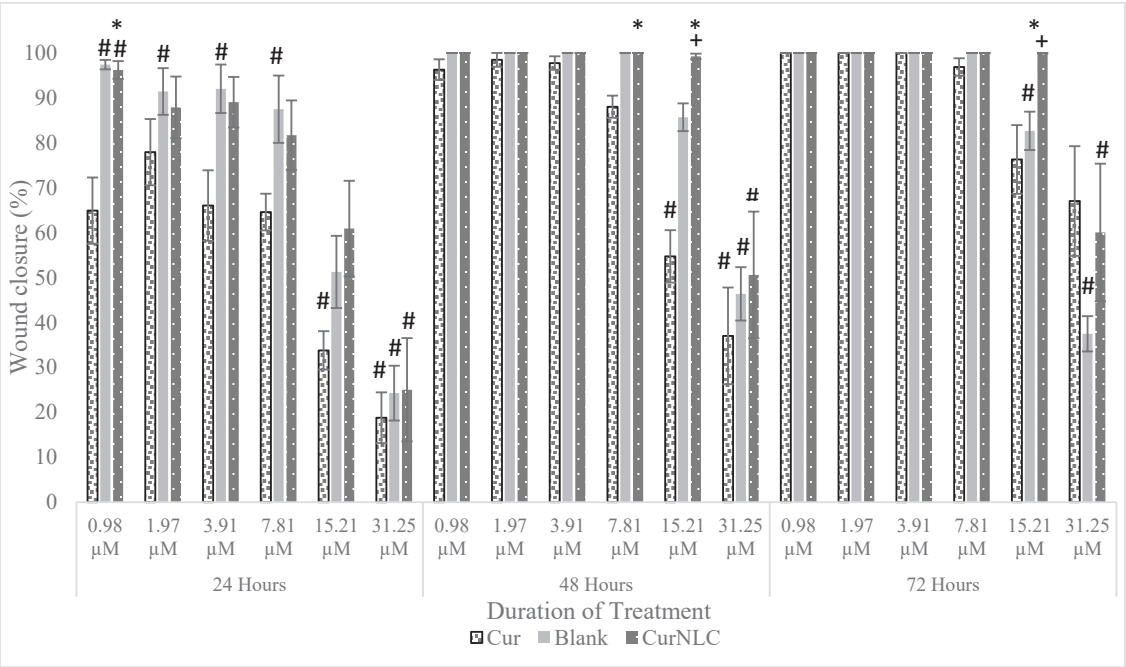


FIGURE 5. Comparison between curcumin-NLC with Curcumin and Blank NLC on wound closure of HaCaT cells treated with 0.98–31.25 µM at 24, 48, and 72 h. #Statistically significant (one-way ANOVA, Tukey's post hoc test, $p<0.05$) compared to respective control. *Statistically significant (independent samples t-test, $p<0.05$) against the respective concentrations of curcumin. +Statistically significant (independent sample t-test, $p<0.05$) against the concentration of Blank NLC. Data expressed as n=4 ±SEM

and 72 h. When compared to curcumin as a control, curcumin-NLC demonstrated a significantly higher rate of wound closure at a concentration of 0.98 µM at 24 h, 7.81 µM and 15.21 µM at 48 h, and 15.21 µM at 72 h. A significant difference between curcumin-NLC and blank NLC was observed at a concentration of 15.21 µM for both 48 and 72 h. This study demonstrated that curcumin-NLCs could enhance the rate of cell migration and wound healing in the HaCaT cell line compared with pure curcumin.

### SKIN IRRITATION STUDY

Skin irritation was assessed visually, with erythema (redness) used as the scoring criterion. Figure 6 shows skin irritation studies of curcumin-NLCs, sodium lauryl sulfate as a positive control, and normal saline as a negative control on the dorsal side of the Sprague–Dawley rats with observation time after application of treatment at 0, 24, 48, and 72 h. The application of curcumin-NLCs did not produce any visible redness or erythema on the

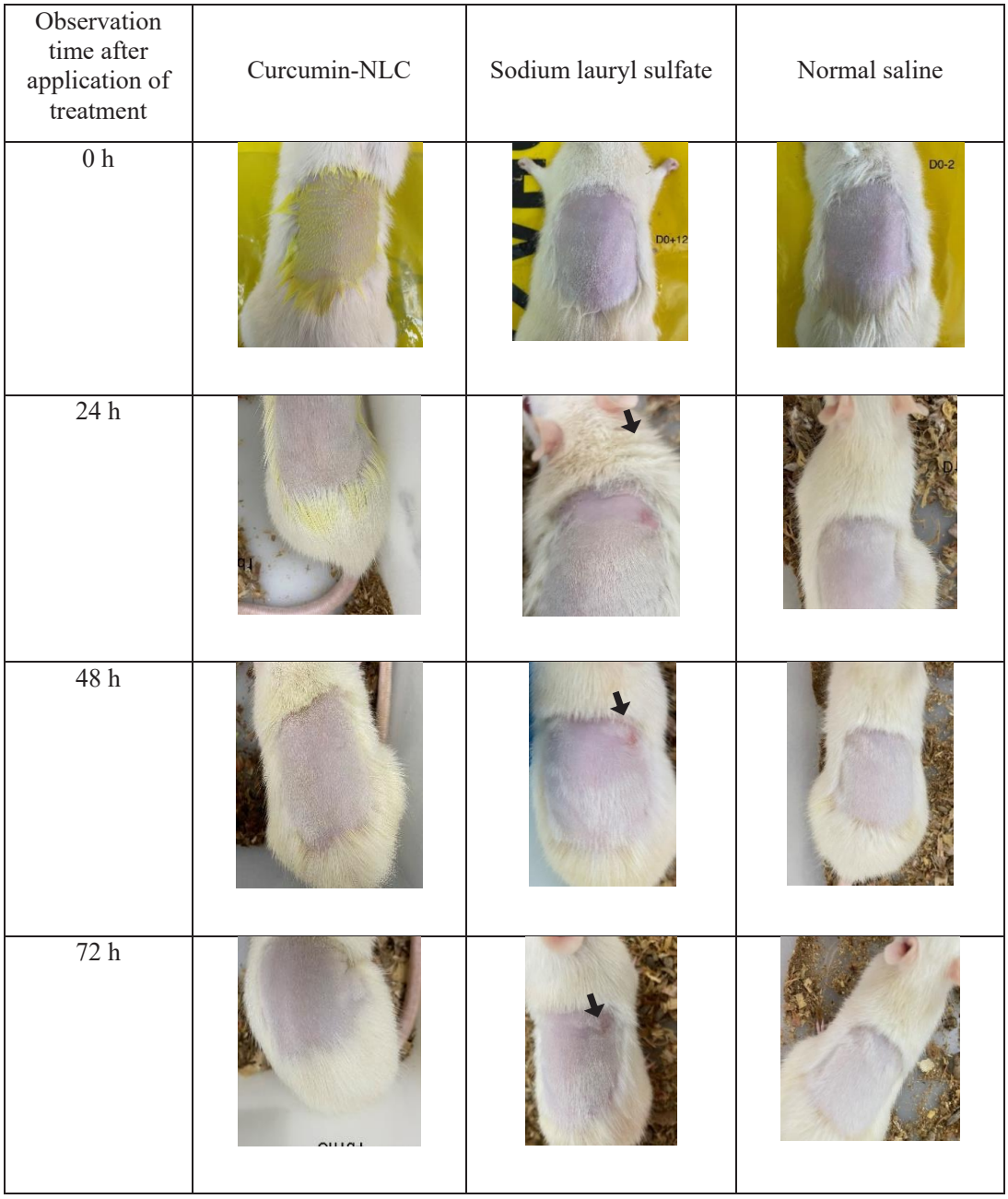


FIGURE 6. Skin irritation studies of curcumin-NLCs, sodium lauryl sulphate (positive control), and normal saline (negative control) as a treatment on the dorsal side of the Sprague–Dawley rat with observation times after application of treatment at 0, 24, 48, and 72 h (n=4). The arrow indicates the presence of the erythema on the rat skin

rat skin compared to sodium lauryl sulfate, which produced well-defined erythema throughout the 72 h. The results suggested that curcumin-NLCs caused no irritation or inflammation, indicating that the formulation was safe for topical application.

## Conclusions

A combination of high shear homogenization and high-pressure homogenization methods was employed to develop an NLC formulation for topical delivery of curcumin. This central composite design was used to optimize the NLC composition, which resulted in a formulation containing 3.5% glyceryl monooleate, 1.5% olive oil, 1% tween 80, and 2% lecithin. This optimized composition produced NLCs with stable physicochemical properties, including a particle size less than 200 nm (ensuring a small and uniform particle size for better skin penetration), a polydispersity index (PDI) less than 0.3 (indicating a narrow size distribution), and a zeta potential (ZP) within the range of -30 to -50 mV (contributing to particle stability). This small and spherical formulation achieved high drug encapsulation and demonstrated a sustained drug release profile that was concentration-dependent. Additionally, it showed improved wound healing activity while maintaining a safe profile, suggesting that curcumin-loaded NLCs could be a viable strategy for treating pressure ulcers.

## Acknowledgements

We would like to thank the Ministry of Higher Education, Malaysia, for providing a research grant under the Fundamental Research Grant Scheme (FRGS/1/2020/SKK0/UKM/02/13).

## References

Akbik, D., Ghadiri, M., Chrzanowski, W. & Rohanizadeh, R. 2014. Curcumin as a wound healing agent. *Life Sciences* 116(1): 1-7. doi:10.1016/j.lfs.2014.08.016

Al-Waeli, A.H.A., Chaichan, M.T., Kazem, H.A. & Sopian, K. 2019. Evaluation and analysis of nanofluid and surfactant impact on photovoltaic-thermal systems. *Case Studies in Thermal Engineering* 13: 100392. doi:10.1016/j.csite.2019.100392

Behbahani, E.S., Ghaedi, M., Abbaspour, M. & Rostamizadeh, K. 2017. Optimization and characterization of ultrasound assisted preparation of curcumin-loaded solid lipid nanoparticles: Application of central composite design, thermal analysis and X-ray diffraction techniques. *Ultrasonics Sonochemistry* 38: 271-280. doi:10.1016/j.ultsonch.2017.03.013

Bhatt, S., Sharma, J.B., Kamboj, R., Kumar, M., Saini, V. & Mandge, S. 2021. Design and optimization of febuxostat-loaded nano lipid carriers using full factorial design. *Turkish Journal of Pharmaceutical Sciences* 18(1): 61-67. doi:10.4274/tjps.galenos.2019.32656

Bhattacharya, S. & Mishra, R. 2015. Pressure ulcers: Current understanding and newer modalities of treatment. *Indian Journal of Plastic Surgery* 48(1): 4-16. doi:10.4103/0970-0358.155260

Borges, A., de Freitas, V., Mateus, N., Fernandes, I. & Oliveira, J. 2020. Solid lipid nanoparticles as carriers of natural phenolic compounds. *Antioxidants* 9(10): 998. doi:10.3390/antiox9100998

Castro, S.R., Ribeiro, L.N.M., Breitkreitz, M.C., Guilherme, V.A., Rodrigues da Silva, G.H., Mitsutake, H., Alcântara, A.C.S., Yokaichiya, F., Franco, M.K.K.D., Clemens, D., Kent, B., Lancellotti, M., de Araújo, D.R. & de Paula, E. 2021. A pre-formulation study of tetracaine loaded in optimized nanostructured lipid carriers. *Scientific Reports* 11(1): 21463. doi:10.1038/s41598-021-99743-6

Chuacharoen, T., Prasongsuk, S. & Sabliov, C.M. 2019. Effect of surfactant concentrations on physicochemical properties and functionality of curcumin nanoemulsions under conditions relevant to commercial utilization. *Molecules (Basel, Switzerland)* 24(15): 2744. doi:10.3390/molecules24152744

Das, S., Ng, W.K. & Tan, R.B.H. 2012. Are nanostructured lipid carriers (NLCs) better than solid lipid nanoparticles (SLNs): Development, characterizations and comparative evaluations of clotrimazole-loaded SLNs and NLCs? *European Journal of Pharmaceutical Sciences* 47(1): 139-151. doi:10.1016/j.ejps.2012.05.010

Elmowafy, M., Samy, A., Raslan, M.A., Salama, A., Said, R.A., Abdelaziz, A.E., El-Eraky, W., El Awdan, S. & Viitala, T. 2016. Enhancement of bioavailability and pharmacodynamic effects of thymoquinone via nanostructured lipid carrier (NLC) formulation. *AAPS PharmSciTech* 17(3): 663-672. doi:10.1208/s12249-015-0391-0

Emami, J., Mohiti, H., Hamishehkar, H. & Varshosaz, J. 2015. Formulation and optimization of solid lipid nanoparticle formulation for pulmonary delivery of budesonide using Taguchi and Box-Behnken design. *Research in Pharmaceutical Sciences* 10(1): 17-33.

Esposito, E., Ravani, L., Mariani, P., Huang, N., Boldrini, P., Drechsler, M., Valacchi, G., Cortesi, R. & Puglia, C. 2014. Effect of nanostructured lipid vehicles on percutaneous absorption of curcumin. *European Journal of Pharmaceutics and Biopharmaceutics* 86(2): 121-132. doi:10.1016/j.ejpb.2013.12.011.

Gatne, M., Tambe, K., Chaudhary, A. & Ravikanth, K. 2015. Acute dermal irritation study of polyherbal gel Mastilep in rabbits. *International Journal of Pharmaceutical Sciences and Research* 6: 3473-3476. doi:10.13040/IJPSR.0975-8232.6(8).3473-76.

Gazori, T., Khoshayand, M.R., Azizi, E., Yazdizade, P., Nomani, A. & Haririan, I. 2009. Evaluation of Alginate/ Chitosan nanoparticles as antisense delivery vector: Formulation, optimization and in vitro characterization. *Carbohydrate Polymers* 77(3): 599-606. doi:10.1016/j.carbpol.2009.02.019

Guhagarkar, S.A., Malshe, V.C. & Devarajan, P.V. 2009. Nanoparticles of polyethylene sebacate: A new biodegradable polymer. *AAPS PharmSciTech* 10(3): 935-942. doi:10.1208/s12249-009-9284-4

Haider, M., Abdin, S.M., Kamal, L. & Orive, G. 2020. Nanostructured lipid carriers for delivery of chemotherapeutics: A review. *Pharmaceutics* 12(3): 288. doi:10.3390/pharmaceutics12030288

Hatcher, H., Planalp, R., Cho, J., Torti, F.M. & Torti, S.V. 2008. Curcumin: From ancient medicine to current clinical trials. *Cellular and Molecular Life Sciences* 65(11): 1631-1652. doi:10.1007/s00018-008-7452-4

Housaindokht, M.R. & Nakhaei Pour, A. 2012. Study the effect of HLB of surfactant on particle size distribution of hematite nanoparticles prepared via the reverse microemulsion. *Solid State Sciences* 14(5): 622-625. doi:10.1016/j.solidstatesciences.2012.01.016

Hussain, Z., Thu, H.E., Ng, S.F., Khan, S. & Katas, H. 2017. Nanoencapsulation, an efficient and promising approach to maximize wound healing efficacy of curcumin: A review of new trends and state-of-the-art. *Colloids and Surfaces B: Biointerfaces* 150: 223-241. doi:10.1016/j.colsurfb.2016.11.036

Kamel, A.E., Fadel, M. & Louis, D. 2019. Curcumin-loaded nanostructured lipid carriers prepared using peceol™ and olive oil in photodynamic therapy: Development and application in breast cancer cell line. *International Journal of Nanomedicine* 14: 5073-5085. doi:10.2147/IJN.S210484

Khor, H.M., Tan, J., Saedon, N.I., Kamaruzzaman, S.B., Chin, A.V., Poi, P.J.H. & Tan, M.P. 2014. Determinants of mortality among older adults with pressure ulcers. *Archives of Gerontology and Geriatrics* 59(3): 536-541. doi:10.1016/j.archger.2014.07.011

Kottner, J., Cuddigan, J., Carville, K., Balzer, K., Berlowitz, D., Law, S., Litchford, M., Mitchell, P., Moore, Z., Pittman, J., Sigaudo-Roussel, D., Yee, C.Y. & Haesler, E. 2020. Pressure ulcer/injury classification today: An international perspective. *Journal of Tissue Viability* 29(3): 197-203. doi:10.1016/j.jtv.2020.04.003

Kumbhar, D.D. & Pokharkar, V.B. 2013. Engineering of a nanostructured lipid carrier for the poorly water-soluble drug, bicalutamide: Physicochemical investigations. *Colloids and Surfaces A: Physicochemical and Engineering Aspects* 416: 32-42. doi:10.1016/j.colsurfa.2012.10.031

Lakhani, P., Patil, A., Taskar, P., Ashour, E. & Majumdar, S. 2018. Curcumin-loaded nanostructured lipid carriers for ocular drug delivery: Design optimization and characterization. *Journal of Drug Delivery Science and Technology* 47: 159-166. doi:10.1016/j.jddst.2018.07.010

Liu, M., Wen, J. & Sharma, M. 2020. Solid lipid nanoparticles for topical drug delivery: Mechanisms, dosage form perspectives, and translational status. *Current Pharmaceutical Design* 26(27): 3203-3217. doi:10.2174/1381612826666200526145706

Mulligan, C.N. 2007. Rhamnolipid biosurfactants: Solubility and environmental issues. In *Thermodynamics, Solubility and Environmental Issues*, edited by Letcher, T.M. Elsevier. pp. 279-298. doi:10.1016/B978-044452707-3/50017-3

Nahak, P., Karmakar, G., Chettri, P., Roy, B., Guha, P., Besra, S.E., Soren, A., Bykov, A.G., Akentiev, A.V., Noskov, B.A. & Panda, A.K. 2016. Influence of lipid core material on physicochemical characteristics of an ursolic acid-loaded nanostructured lipid carrier: An attempt to enhance anticancer activity. *Langmuir* 32(38): 9816-9825. doi:10.1021/acs.langmuir.6b02402

Pradhan, M., Singh, D., Murthy, S.N. & Singh, M.R. 2015. Design, characterization and skin permeating potential of Fluocinolone acetonide loaded nanostructured lipid carriers for topical treatment of psoriasis. *Steroids* 101: 56-63. doi:10.1016/j.steroids.2015.05.012

Puglia, C., Frasca, G., Musumeci, T., Rizza, L., Puglisi, G., Bonina, F. & Chiechio, S. 2012. Curcumin loaded NLC induces histone hypoacetylation in the CNS after intraperitoneal administration in mice. *European Journal of Pharmaceutics and Biopharmaceutics* 81(2): 288-293. doi:10.1016/j.ejpb.2012.03.015

Rahman, H.S., Rasedee, A., How, C.W., Abdul, A.B., Zeenathul, N.A., Othman, H.H., Saeed, M.I. & Yeap, S.K. 2013. Zerumbone-loaded nanostructured lipid carriers: Preparation, characterization, and antileukemic effect. *International Journal of Nanomedicine* 8: 2769-2781. doi:10.2147/IJN.S45313

Rapalli, V.K., Kaul, V., Waghule, T., Gorantla, S., Sharma, S., Roy, A., Dubey, S.K. & Singhvi, G. 2020. Curcumin loaded nanostructured lipid carriers for enhanced skin retained topical delivery: optimization, scale-up, *in-vitro* characterization and assessment of *ex-vivo* skin deposition. *European Journal of Pharmaceutical Sciences* 152: 105438. doi:10.1016/j.ejps.2020.105438

Soleimanifard, M., Sadeghi Mahoonak, A., Ghorbani, M., Heidari, R. & Sepahvand, A. 2020. The formulation optimization and properties of novel oleuropein-loaded nanocarriers. *Journal of Food Science and Technology* 57(1): 327-337. doi:10.1007/s13197-019-04065-1

Sreedharan, S.M. & Singh, R. 2019. Ciprofloxacin functionalized biogenic gold nanoflowers as nanoantibiotics against pathogenic bacterial strains. *International Journal of Nanomedicine* 14: 9905-9916. doi:10.2147/IJN.S224488

Szutkowski, K., Kołodziejska, Z., Pietralik, Z., Zhukov, I., Skrzypczak, A., Materna, K. & Kozak, M. 2018. Clear distinction between CAC and CMC revealed by high-resolution NMR diffusometry for a series of bis-imidazolium gemini surfactants in aqueous solutions. *RSC Advances* 8(67): 38470-38482. doi:10.1039/c8ra07081d

Toden, S., Okugawa, Y., Jascur, T., Wodarz, D., Komarova, N.L., Buhrmann, C., Shakibaei, M., Boland, C.R. & Goel, A. 2015. Curcumin mediates chemosensitization to 5-fluorouracil through miRNA-induced suppression of epithelial-to-mesenchymal transition in chemoresistant colorectal cancer. *Carcinogenesis* 36(3): 355-367. doi:10.1093/carcin/bgv006

Vijayakumar, A., Baskaran, R., Baek, J-H., Sundaramoorthy, P. & Yoo, B.K. 2019. *In vitro* cytotoxicity and bioavailability of ginsenoside-modified nanostructured lipid carrier containing curcumin. *AAPS PharmSciTech* 20(2): 88. doi:10.1208/s12249-019-1295-1

Westby, M.J., Dumville, J.C., Soares, M.O., Stubbs, N., Norman, G. & Foley, C.N. 2015. Dressings and topical agents for treating pressure ulcers. *Cochrane Database of Systematic Reviews* 6(6): CD011947. doi:10.1002/14651858.CD011947

Wissing, S.A., Kayser, O. & Müller, R.H. 2004. Solid lipid nanoparticles for parenteral drug delivery. *Advanced Drug Delivery Reviews* 56(9): 1257-1272. doi:10.1016/j.addr.2003.12.002

Yang, G., Wu, F., Chen, M., Jin, J., Wang, R. & Yuan, Y. 2019. Formulation design, characterization, and *in vitro* and *in vivo* evaluation of nanostructured lipid carriers containing a bile salt for oral delivery of gypenosides. *International Journal of Nanomedicine* 14: 2267-2280. doi:10.2147/IJN.S194934

*Corresponding author; email: email: hanifzulfakar@ukm.edu.my


FIGURE S1. Curcumin NLC for 17 experimental formulations

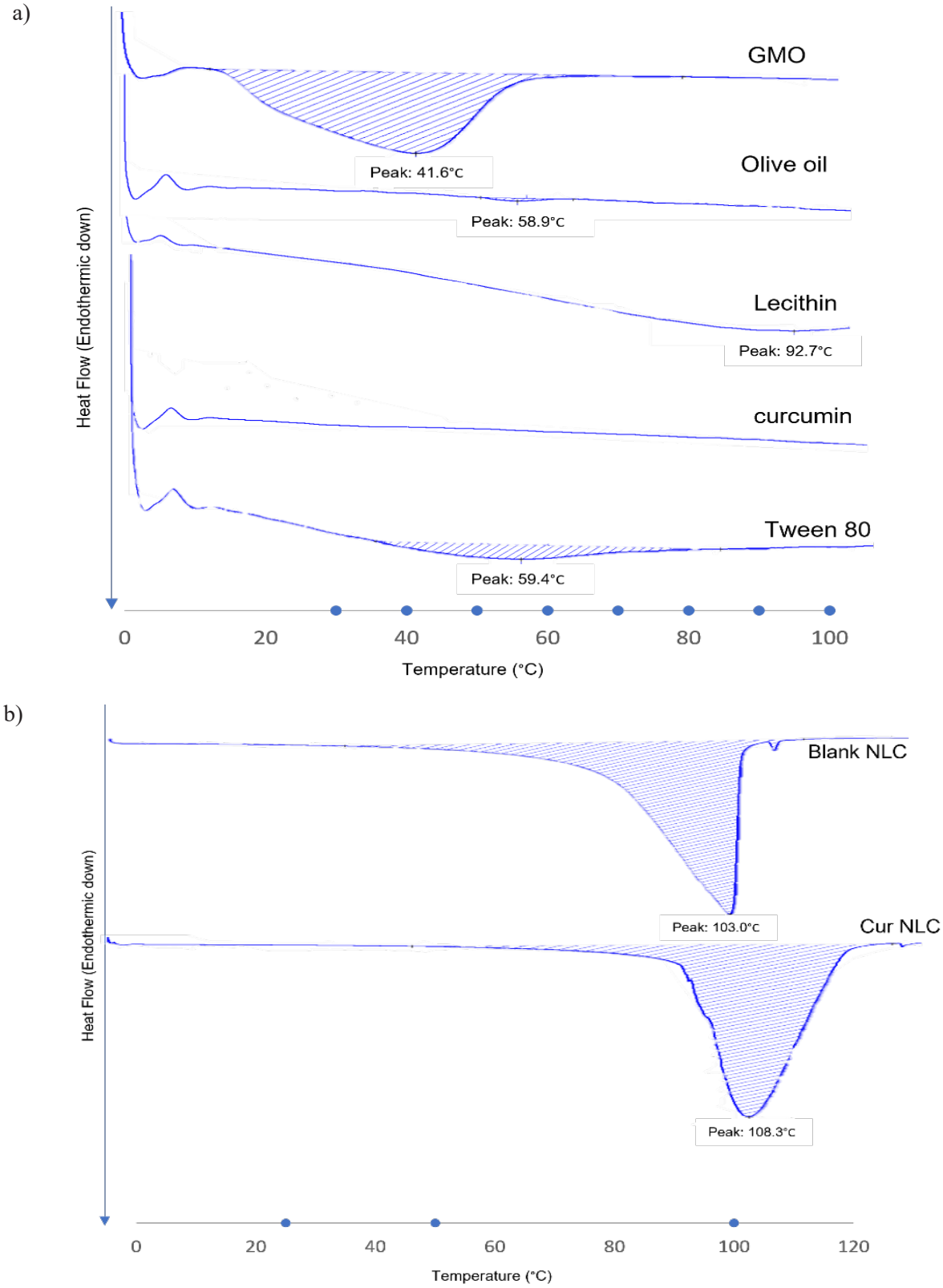


FIGURE S2. DSC thermograms of a) NLC component and b) blank NLC and cur NLC

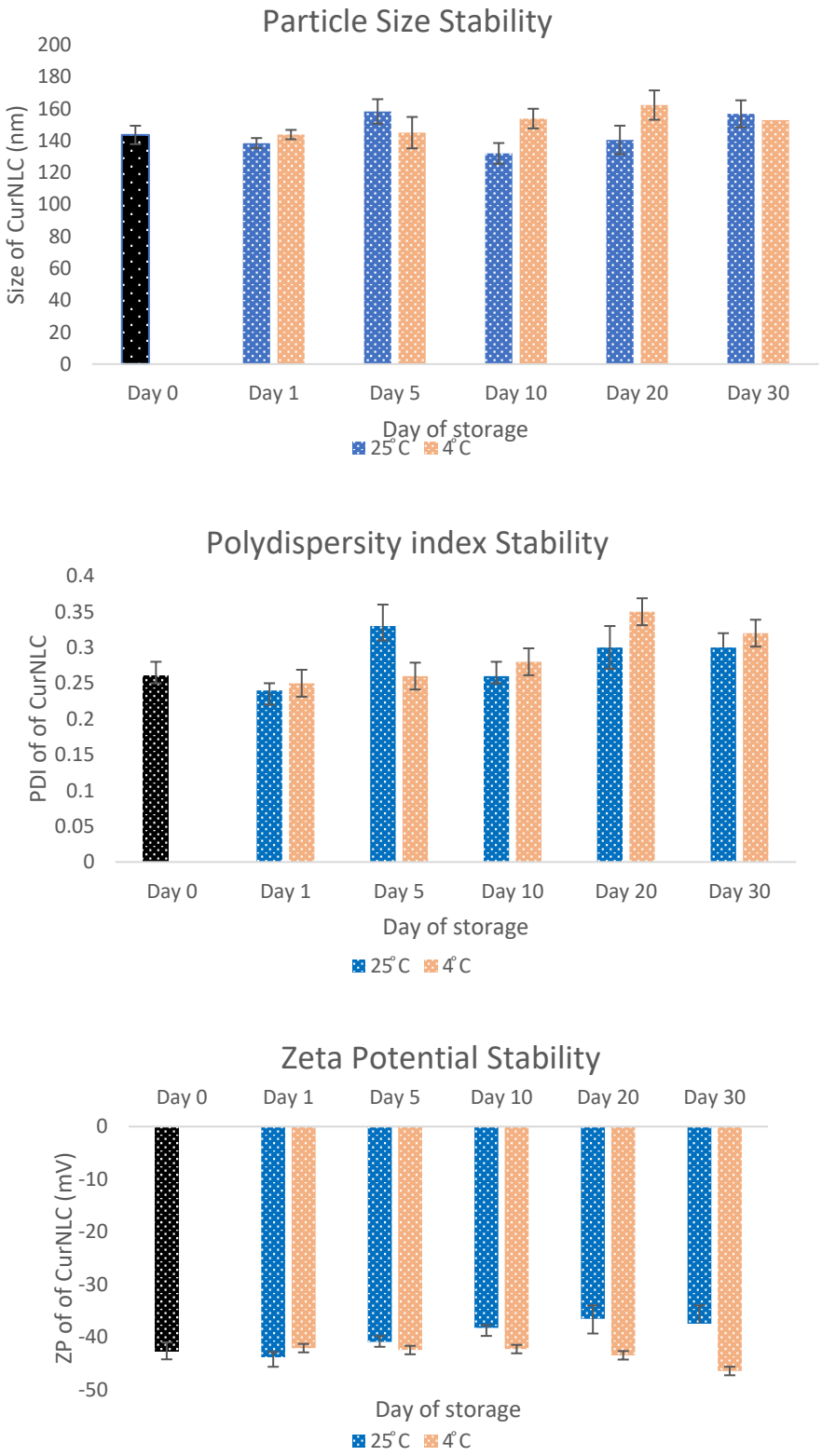


FIGURE S3. The stability of curcumin-NLC for day 0, 1, 5, 10, 20 and 30 at 4 and 25°C a) Particle size stability b) Polydispersity index stability c) Zeta potential stability. Data

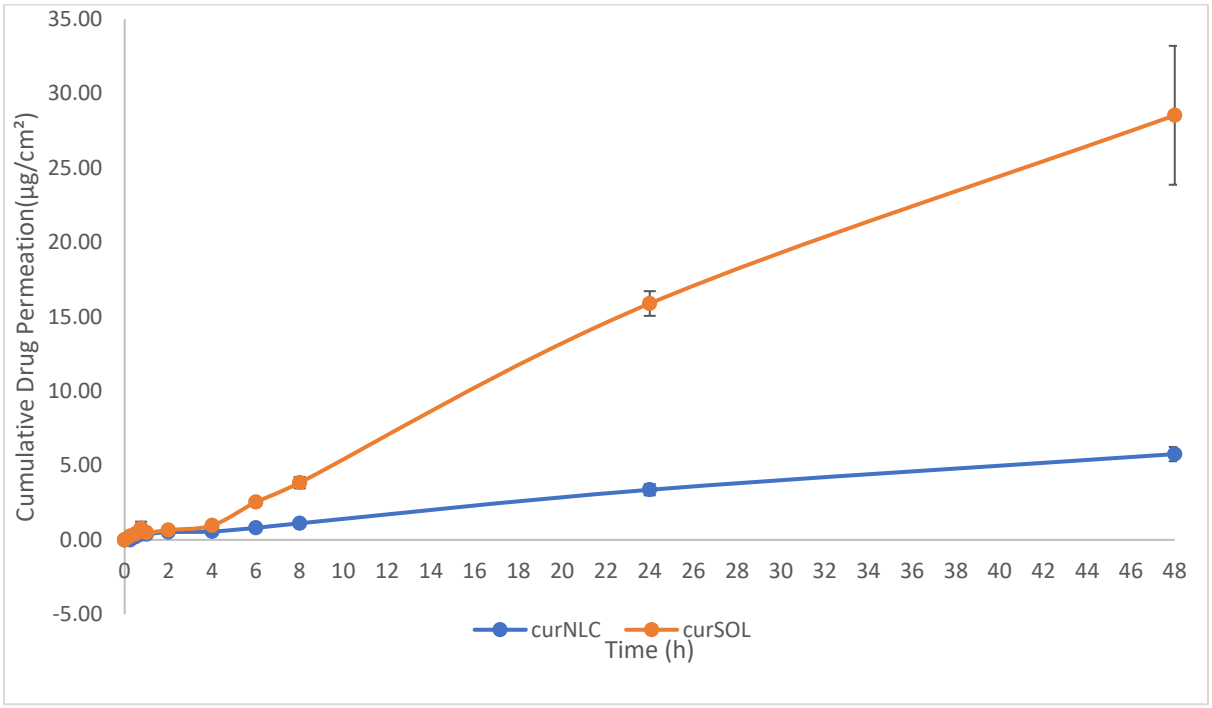


FIGURE S4. *In-vitro* permeation profile of curcumin solution and curcumin NLC dispersion (Mean ± SEM, n= 3)